

Adsorption of Nitric Oxide on Tin Oxide

MIKI NIWA, TAKASHI MINAMI, HITOSHI KODAMA, TADASHI HATTORI,
AND YUICHI MURAKAMI

*Department of Synthetic Chemistry, Faculty of Engineering,
Nagoya University, Furo-cho, Chikusa-ku, Nagoya 464, Japan*

Received August 16, 1977; revised February 7, 1978

Adsorption of NO on evacuated SnO₂ was investigated to know adsorbed species and available active sites. On deeply reduced sites, adsorbed NO was decomposed into N₂ and N₂O even at room temperature to oxidize these sites by the incorporation of oxygen atoms. A chelating NO₂ compound which consisted of surface oxygen and adsorbed NO was found on the transient-reduced sites. Furthermore, NO radical and Sn(NO)₂ were detected as reversibly adsorbed species on oxidized SnO₂. The NO radical may be weakly coordinated to the Sn⁴⁺ ion in the low concentration of adsorbed molecules, but further adsorption of NO allowed the radical to be coupled to form Sn(NO)₂.

INTRODUCTION

A considerable amount of research has been devoted to the detection and characterization of adsorbed species of nitric oxide by use of ir and ESR spectroscopies. In particular, infrared study seems to be the most powerful to examine the adsorbed state of NO and available active sites. Various types of adsorbed species are known at present as a result of investigations on this subject since the pioneering work of Terenin and Roev (1). More recently, adsorbed NO molecules and modes of bonding with surface sites have been described in detail on some adsorbents such as Cr₂O₃/SiO₂ (2), Rh/Al₂O₃ (3), ion-exchanged zeolites (4), and so forth.

On the other hand, adsorbed NO radicals have been detected on such solids as MgO (5), Al₂O₃ (6), ZrO₂, CeO₂, and ThO₂ (7). Nitric oxide has also been characterized as being paramagnetic in the gas phase. The ESR spectrum of this gaseous molecule

is not detected, however, because the spin magnetic momentum is exactly canceled out by the orbital magnetic momentum. The adsorbed NO radical is observed by a usual X-band spectrometer only in the adsorbed state because the orbital magnetic momentum is quenched by the surface field. Such a NO radical is weakly held on the surface and possesses a hyperfine structure due to the nuclear spin of nitrogen. Otherwise, nitrosyl complex, which consists of coordinated NO and metal ion, is also detected by ESR. The structure and reactivity of such nitrosyl complexes have been investigated by Lunsford *et al.* (8, 9).

Metal oxide catalysts used in the reduction of NO seem to have a surface with various oxidation states depending on the reaction conditions. It is interesting to know the adsorbed species and these available adsorption sites, and in addition to correlate such a profile of adsorption with the reaction. The purpose of this study was

to identify the adsorbed species and the available active sites on SnO_2 with various oxidation states of the surface by gravimetric, ir, and ESR measurements.

EXPERIMENTAL METHODS

Sample. The SnO_2 sample was prepared by pressing SnO_2 powder, followed by crushing (28–48 mesh) and calcinating at 450°C in the air stream. In an X-ray diffraction pattern of the sample, only SnO_2 was detected. The $\text{SnO}_2/\text{SiO}_2$ sample was prepared by an impregnation of silica gel Pore Dia 70 (Dokai Chemical Ind.) in a stannous chloride solution, followed by drying and calcinating at 500°C for 4 hr in an air stream. The tin oxide content was 5 wt%. Nitric oxide was supplied by Takachiho Chemical Ind. Co. Ltd., and used after vacuum distillation.

Gravimetric adsorption measurements. A gravimetric adsorption experiment was performed by using a quartz spring balance with a force constant of 20.7 mg/cm . A sample of known weight (about 150 mg) was suspended in a vessel, the vessel was evacuated at a temperature above 350°C , and then the extension of the spring accompanied with adsorption was monitored by a traveling microscope. The quartz spring was hung in a double-sealed Pyrex glass tube the outer tube of which was filled with CCl_4 vapor to keep a constant temperature. A portion of the gas phase was sampled for analysis in a gas chromatograph with silica gel for N_2O and a 13X molecular sieve for O_2 , N_2 , and NO at room temperature.

Infrared measurements. Infrared spectra were recorded on a Jasco IR-G spectrometer in the region of 4000 to 400 cm^{-1} . The SnO_2 sample was pressed into a disk 20 mm in diameter under a pressure of 6 to 7 tons/cm². A pellet holder was hung in a Pyrex glass cell by a platinum wire. The sample was evacuated at 400°C in the upper furnace part of the cell, and it

was then lowered to adsorb NO gas and expose the ir beam at room temperature.

ESR measurements. The sample was placed in Pyrex glass or quartz ampoule for ESR measurements and dehydrated at 250°C at atmospheric pressure, followed by evacuation for 1 hr under a vacuum of 10^{-3} Torr. Nitric oxide was introduced at room temperature, and after 30 min ESR measurements of the sample were made. ESR measurements were made at 77 and 162 K with a JEOL spectrometer (JES-ME-1X). The g -values and hyperfine splitting constants were calculated by comparison with the value for the Mn^{2+} impurity in MgO. The radical concentrations were determined by using a coke sample diluted with KBr as the standard.

RESULTS

Gravimetric Adsorption Measurements

The amounts of NO adsorption on SnO_2 evacuated and further treated by hydrogen and oxygen were evaluated using a quartz spring microbalance. Increases in weight were measured after allowing the sample to stand for about 10 min at each partial pressure of NO (Fig. 1), because rate of NO adsorption was very slow (10) and it was difficult to attain an adsorption equilibrium. The partial pressure of NO was increased up to about 100 Torr (following the arrow in Fig. 1), and then gaseous NO was fully evacuated. In all the cases, adsorbed materials were irreversibly held on the surface and hardly desorbed by the vacuum evacuation.

Simultaneously, gas in the vessel was analyzed by gas chromatography, and it was found that N_2O and N_2 were formed upon adsorption of NO at room temperature. No molecular oxygen was detected in the gas phase so that the oxygen atoms were certainly adsorbed on the surface. Therefore, it is clear that the expansion of microbalance is due to not only adsorbed NO but also to oxygen on the surface.

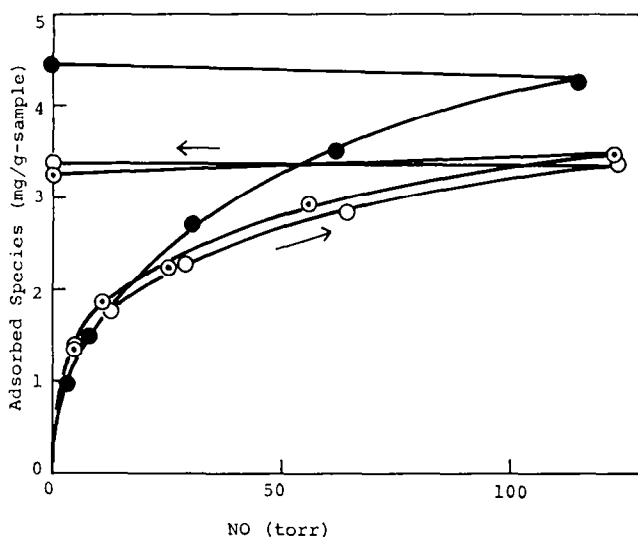


FIG. 1. Variation of adsorbed amount with different partial pressures of NO at room temperature on SnO₂ evacuated (⊙) and further treated with hydrogen (●) and oxygen (○) at 450°C.

Table 1 summarizes the amounts of N₂ and N₂O formed and of oxygen atoms and of NO molecules adsorbed when NO was adsorbed at 100 Torr on the SnO₂ which was variously evacuated and treated. The amount of adsorbed oxygen atoms was evaluated from N₂ and N₂O formed, and the amount of adsorbed NO molecules was calculated from the adsorbed oxygen and total increase in weight.

As shown in Table 1, the reduction of SnO₂ by hydrogen increased the dissocia-

tion of NO but decreased the adsorption of NO molecules. This fact shows clearly that dissociative adsorption of NO, at least, takes place on reduced sites of SnO₂. On the other hand, treatment with oxygen did not influence the adsorbing property as much. It seems that oxygen was desorbed by the evacuation at 450°C after treatment with oxygen.

Dependence of such an adsorption profile on evacuation temperature was also examined. As shown in Table 1, elevation of

TABLE 1
N₂ and N₂O Formed and O and NO Adsorbed on SnO₂ at Room Temperature^a

| Evacuation temperature (°C) | Treatment ^b | N ₂ | N ₂ O | NO dissociated (μmol/g of sample) | O adsorbed | NO molecular adsorbed |
|-----------------------------|------------------------|----------------|------------------|-----------------------------------|------------|-----------------------|
| 450 | — | 6.2 | 9.1 | 30.4 | 21.4 | 100 |
| 450 | O ₂ | 6.0 | 12.4 | 36.7 | 24.3 | 103 |
| 450 | H ₂ | 38.8 | 96.5 | 271 | 174 | 55.2 |
| 350 | — | 2.4 | 4.6 | 14 | 9.4 | 76 |
| 400 | — | 4.6 | 5.9 | 21 | 15 | 96 |
| 500 | — | 8.1 | 14.7 | 45.6 | 30.9 | 149 |

^a Evacuated for 1 hr.

^b Treated with oxygen or hydrogen on evacuated sample for 30 min, followed by evacuation for 15 min at 450°C.

evacuation temperature resulted in an increase of adsorption of NO irrespective of the type of adsorption.

Infrared Spectra of Adsorbed NO

Identification of the adsorbed species of NO on evacuated SnO₂ was attempted by ir spectroscopy. The adsorption of NO at 100 Torr on SnO₂ evacuated at 400°C

for 1 hr revealed the spectrum shown in Fig. 2, trace b in the presence of gaseous NO. It contained absorption bands at 1910, 1830, 1290, and 1175 cm⁻¹. An absorption band at 1250 cm⁻¹ was caused by contamination of a KBr window with silicone grease. Evacuation of gaseous NO diminished the 1910- and 1830-cm⁻¹ bands,

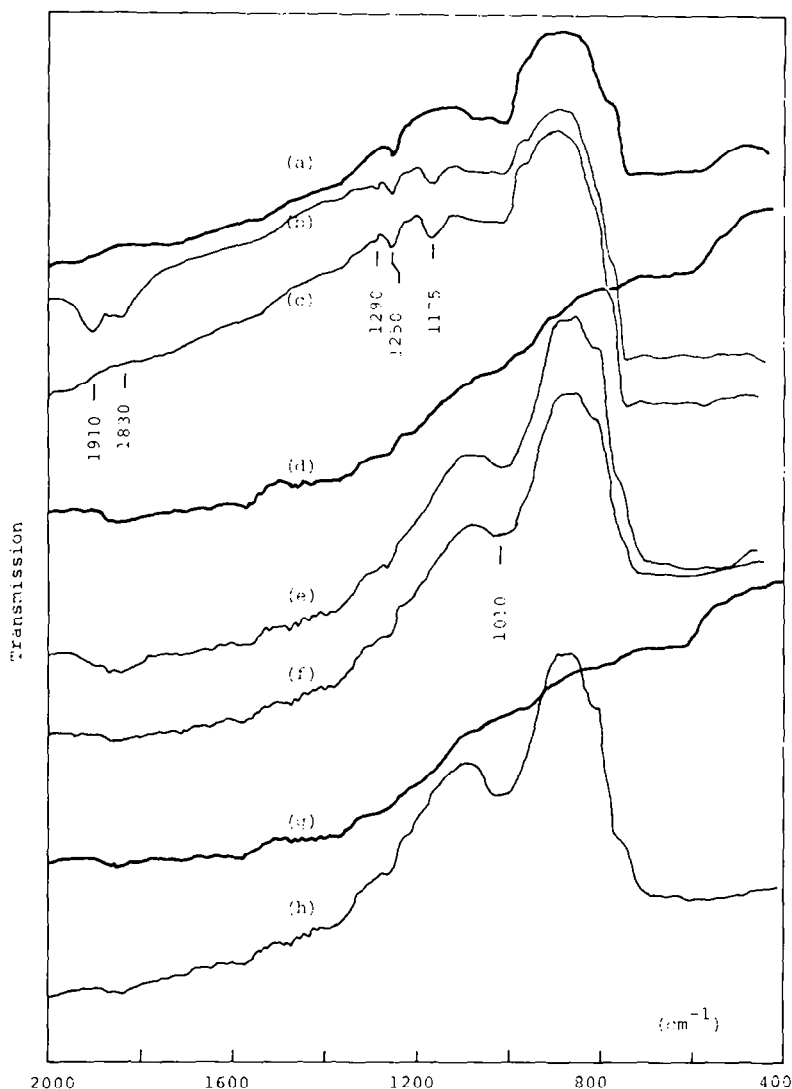


FIG. 2. The ir spectra on SnO₂: (a) evacuation at 400°C for 1 hr; (b) admission of NO at 100 Torr; (c) evacuation; (d) re-evacuation at 400°C for 2 hr; (e) admission of NO at 100 Torr; (f) evacuation; (g) re-evacuation at 400°C for 1 hr; (h) admission of oxygen at 43 Torr followed by evacuation.

bands, as shown in Fig. 2, trace c. This sample was further evacuated at 400°C for 2 hr and subjected to additional measurements. Well evacuation of the sample diminished the absorption below 800 cm^{-1} which is observed in the background of SnO_2 in Fig. 2, trace a. However, this band was recovered by the adsorption of NO, and in addition also an absorption at band 1010 cm^{-1} became clear (Fig. 2, trace e). The intensities of the 1010- cm^{-1} and 700- to 400- cm^{-1} absorption bands were not decreased by the evacuation of gas phase at all, but these were removed by re-evacuation at 400°C for 1 hr, and the background spectrum was obtained, as shown in Fig. 2, trace g. Adsorption of oxygen on this sample followed by evacuation revealed the spectrum shown in Fig. 2, trace h which was exactly the same as that obtained by the adsorption of NO. It has already been reported that various structures of a tin oxide compound revealed absorptions due to Sn-O bond in the region below 800 cm^{-1} (11). Consequently, the 1010- cm^{-1} and 700- to 400- cm^{-1} bands are based on the oxygen at the surface. In other words, the surface of SnO_2 is oxidized by the adsorption of NO at room temperature; this is in accord with the facts of the quantitative study shown above.

The absorptions at 1290 and 1175 cm^{-1} were observed in the case of evacuation

for 1 hr, but not on the well-evacuated sample. It is therefore proposed that the bands appear in the adsorption of the transient-reduced surface. This proposal is supported by the fact that such absorptions were observable in the case of the middle level of the 700- to 400- cm^{-1} absorption band which is indicative of an Sn-O bond. Recent investigation by Kugler *et al.* (12) showed that NO is adsorbed on the reduced sample of Cr_2O_3 as a chelating NO_2 species. The observed bands at 1285 cm^{-1} (w) and 1180 cm^{-1} (s) were due to the symmetric and asymmetric modes of the chelating NO_2 species which consisted of the adsorbed NO and surface oxygen. The bands observed here at 1290 and 1175 cm^{-1} may be ascribed to such symmetric and asymmetric stretching vibrations of the chelating NO_2 species. Well evacuation of the surface reduced the oxygen-containing sites as judged by the decrease in the intensity of bands below 700 cm^{-1} and probably stimulated the formation of N_2 and N_2O on the reduced sites. The intensity of nitrate bands may be so weak that the ir spectrum is observable only in the transient-reduced state.

The absorptions at 1910 and 1830 cm^{-1} are not ascribable to two different species but to an identical adsorbed species, because the intensities of these bands have a linear relationship as shown in

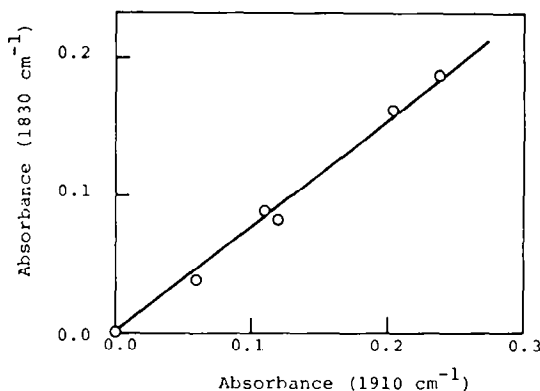


FIG. 3. Linear relationship between adsorbances at 1910 and 1830 cm^{-1} .

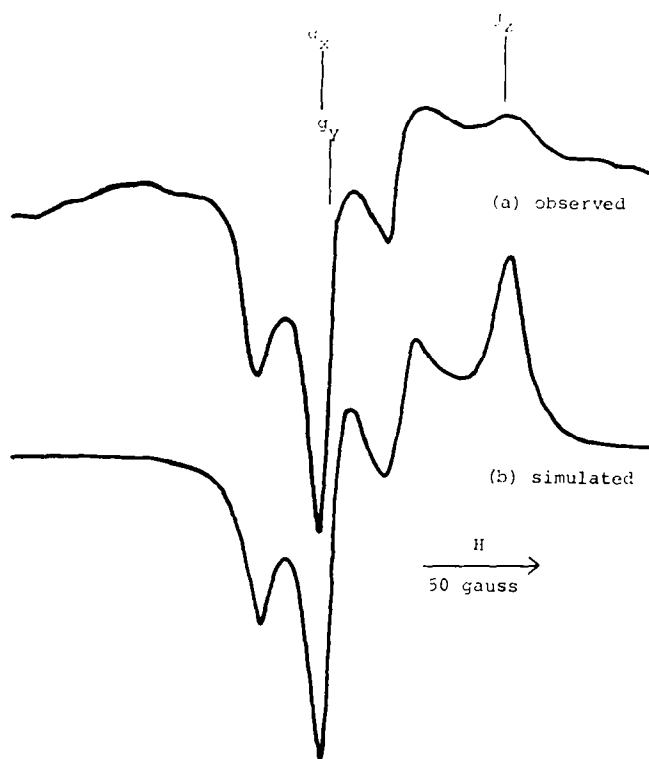


FIG. 4. ESR spectra of adsorbed NO on SnO_2 : (a) observed, (b) simulated.

Fig. 3. By analogy with $[\text{Co}(\text{NO})_2]^{2+}$, as reported by Windhorst and Lunsford (4), the absorptions at 1910 and 1830 cm^{-1} can be due to the asymmetric and symmetric stretching vibrations of $\text{Sn}(\text{NO})_2$.

ESR Measurements

The typical ESR spectrum of nitric oxide adsorbed on evacuated SnO_2 is shown in Fig. 4, trace a. This spectrum exhibits hyperfine structures (hfs) due to the nuclear spin of nitrogen and is very similar to those obtained on ZnS by Lunsford (13), TiO_2 by Imelik *et al.* (14), and cation-exchanged zeolites by Kasai and Bishop (15). These were not observed at room temperature and were easily removed by a short evacuation, which is in accord with the results on other adsorbents previously investigated.

Kasai and Bishop (15) reported the analysis of the ESR spectrum of adsorbed

NO by a computer simulation and determined that $g_x \neq g_y \neq g_z$, and $a_y \neq a_x = a_z \approx 0$. According to Kanzig and Cohen (16), E (energy width between levels of $2p\pi$ and $2p\sigma$) is approximately equal to $2\lambda/(g_x - g_y)$ ($\lambda = 0.015$ eV for NO), and so g_x is never equal to g_y . In such observed spectra, however, g_x is nearly the same as g_y , as described below. It is therefore not easy to determine rigorously the hfs constants. In this paper, these hfs constants were determined to fit the simulated spectrum to the observed one by the nonlinear least squares method (20). The computation was performed with a FACOM 230-60 in Nagoya University Computation Center.

The obtained g -value and hfs constants are listed in Table 2, and the simulated spectra nearly coincided with the experimentally observed one, except for a high-field maximum. Such a procedure for

TABLE 2
g-Values and hfs Constants

| Adsorbent | g_x | g_y | g_z | a | | | w^a |
|-----------------------------|-------|-------|-------|-------|-------|-------|-------|
| | | | | a_x | a_y | a_z | |
| SnO_2 | 2.001 | 1.999 | 1.95 | 0 | 31.0 | 0 | 8.81 |
| $\text{SnO}_2/\text{SiO}_2$ | 2.002 | 2.002 | 1.94 | 0 | 28.2 | 0 | 6.73 |

^a Line width.

determining the parameter was applied to a similar spectrum from a sample adsorbed on $\text{SnO}_2/\text{SiO}_2$. It can be found from Table 2 that g_x is greater than g_y by 0.002 for SnO_2 and only by less than 0.0001 for $\text{SnO}_2/\text{SiO}_2$.

As previously indicated by Lunsford (5), NO is frozen at 77 K, so that all of the sealed NO may be essentially adsorbed on the surface of samples. It follows that the radical concentration measured at liquid nitrogen temperature may not be affected by the partial pressure of NO but by the total amount of sealed NO. This was experimentally confirmed by the use of ampoules of different volumes. When NO was introduced into ampoules of different volumes at a constant partial pressure, different amounts of NO radical were observed. On the other hand, even at different partial pressures, a consistent radical concentration was obtained only by admission of a fixed amount of NO. At temperatures above 122 K, the boiling point of NO, however, the radical concentration was influenced by the partial pressure.

The concentration of NO radical on SnO_2 at 77 K had a sharp maximum with respect to the amount of NO sealed. It increased in a small amount of sealed NO, but decreased when over 1×10^{20} molecules per gram of SnO_2 of NO were introduced. Such a decrease in the radical concentration does not come from the condensation as in the liquid state, because at 162 K, above the boiling point of NO, the radical concentration reaches the maximum value

with respect to the partial pressure of NO, as shown in Fig. 5. The radical concentration was at most 0.05 times as much as the sealed NO.

The variation of the radical concentration with the evacuation temperature was then measured. Because the radical concentration was suppressed by the excess adsorption of NO, measurements were done with admission of small amounts of NO. As shown in Fig. 6, the radical concentration was affected by the evacuation temperature and reached the maximum at about 450°C, but surface area was nearly constant. Furthermore, various treatments on the evacuated sample have been carried out for 30 min, followed by re-evacuation for 15 min at each temperature, as in the gravimetric adsorption measurements. As shown in Fig. 6, reduction or hydration of the evacuated sample markedly reduced the radical concentration, whereas oxidation increased it except at about 450°C. The tin oxide evacuated and further oxidized at 450°C followed by re-evacuation at 500°C exhibited greater amounts of NO radical than the one only evacuated. It may be therefore surmised that oxygen adsorbed at about 450°C not only oxidizes the sample surface but interacts with NO

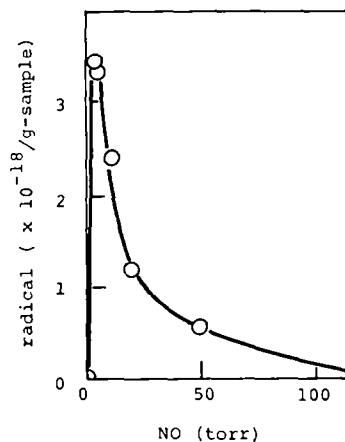


FIG. 5. Dependence of radical concentration on partial pressure at 162 K on SnO_2 evacuated at 450°C.

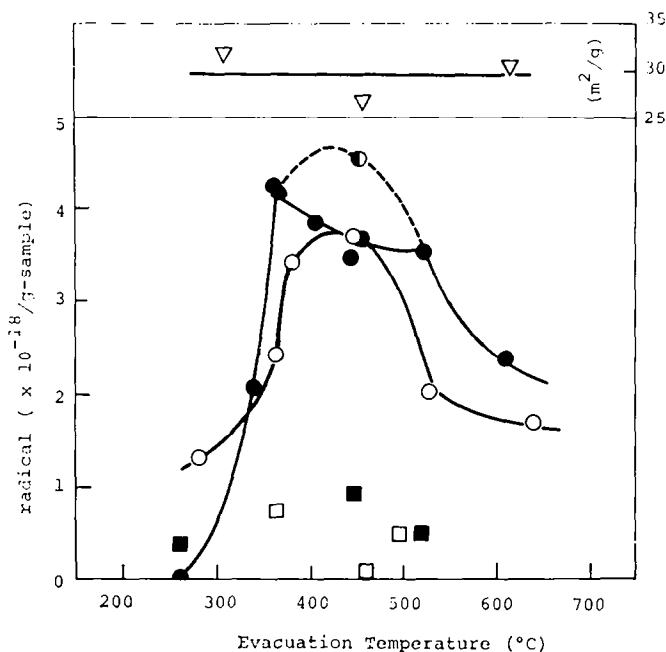


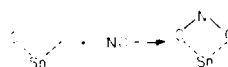
FIG. 6. Variation of radical concentration with evacuation temperature (○) and further treatment at different temperatures with oxygen (●), hydrogen (■), and water vapor (□) in the addition of 7.6×10^{18} NO molecules per gram of SnO₂, and variation in surface area of evacuated sample (▽). (●) shows the result of the procedure in which the evacuated sample is oxidized at 450°C, followed by re-evacuation at 500°C.

to suppress the formation of NO radical. As is easily understood, such a variation in the radical concentration with various treatments is directly contrary to that observed in the gravimetric adsorption measurements. The reduction of oxide stimulated irreversible adsorption as well as decomposition into N₂ and N₂O, but on the contrary suppressed the radical adsorption. Moreover, evacuation at a temperature above 450°C further increased the adsorption of NO, but decreased the paramagnetic adsorbed NO.

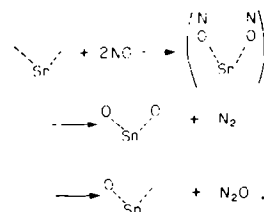
DISCUSSION

Findings in this communication show that a few kinds of adsorbed species of NO exist on the surface. It may be appeared that the profile of these adsorbed species is correlated well with the oxidation state of SnO₂. Solymosi and Kiss (10) have observed that rate and extent of

adsorption of NO were exceedingly high on reduced SnO₂ and surmised the formation of adsorbed NO. The quantitative facts in this paper are in good agreement with data in their communication. The adsorbed species of NO, however, is not a NO⁻ species bonded to a metal ion but probably the chelating NO₂, described as follows:

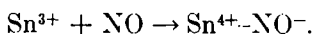


Adsorption of deeply reduced sites leads to the formation of N₂ and N₂O even at room temperature, i.e.,



Oxidation of sites by adsorption of NO was visualized by the appearance of Sn-O bond in the region below 1100 cm^{-1} , as shown above. This scheme of NO decomposition leads us to suspect that NO-CO and NO-H₂ reactions on SnO₂ proceed via the oxidation-reduction mechanism, as do other oxides (17-19). According to Solymosi and Kiss (10), the decomposition of NO proceeded only at temperatures above 100°C unlike our observations. The low activity of the SnO₂ used by them is probably due to the method of preparation.

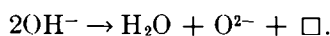
It is well known that the bond strength of N-O is somewhat weakened in the anion form, and therefore it is probably easily decomposed into N₂ and N₂O. It is reasonable to regard the NO⁻ ion as the intermediate species adsorbed and decomposed on reduced sites. From such a point of view, the metal ions which accommodate for the NO adsorption are considered to be low valence ions such as Sn³⁺ or Sn²⁺, although these have not been rigorously identified. Like the study of NO adsorption on TiO₂ (14), electron transfer from a metal ion to adsorbed NO may occur in association with the adsorption. If the active site is regarded as an Sn³⁺ ion, a plausible reaction step, in the first place, is described as



Adsorbed NO⁻ ions have the bent-form structure and probably interact each other to form N₂ and N₂O.

On the other hand, the NO radical and Sn(NO)₂ were observed as the reversible adsorbed species. However, the concentration of these reversible adsorbed species is very low in comparison with adsorbed chelating NO₂ or trapped oxygen atom. When comparison was made between variations in amounts of adsorbed radical and irreversibly adsorbed species, contrary trends were found. The radical concentration decreased with the reduction of sites by hydrogen in direct contrast with that

of irreversibly adsorbed species. It is therefore surmised that the paramagnetic species is adsorbed on the oxidized sites. The increase of the NO radical by evacuation below 450°C may be based on the increase in the concentration of the bare Sn⁴⁺ ion due to the dehydration of the surface. The inhibition of radical formation by the rehydration gives support to this consideration. These sites may be called the anion vacancy neighboring the Sn⁴⁺ ion which can be described as



Evacuation at temperatures above 450°C results in the deep reduction of the surface and an increase in the concentration of reduced sites. The predominance of reduced sites on the surface certainly stimulates the adsorption of NO on reduced sites but inhibits the formation of the NO radical. Contrary trends in the influence of evacuation temperature on the radical and the irreversible adsorptions can be explained by such a variation in the surface component.

As observed above, the formation of NO radical was decreased by the adsorption of a great amount of NO. This suggests a dipolar interaction between adsorbed radicals, and furthermore, the formation of other species in place of the radical. The irreversibly adsorbed molecules, however, can be disregarded, because these seem to be adsorbed on reduced sites. On the contrary, Sn(NO)₂ is reversibly adsorbed and dependent on the partial pressure of NO, as is the NO radical. The Sn(NO)₂ species seems to be diamagnetic, because neighboring molecules interact with each other, and to lose its paramagnetic susceptibility. In dilute concentrations of adsorbed NO, each molecule on the Sn⁴⁺ site exhibits the paramagnetic property. An increase in adsorbed NO makes the radical saturated on the Sn⁴⁺ site, and these may interact with each other and couple to form Sn(NO)₂. Probably, this

dimeric species is coordinated to the Sn^{4+} ion and can be regarded as a nitrosyl complex $[\text{Sn}(\text{NO})_2]^{4+}$.

ACKNOWLEDGMENT

This work was partially supported by a Grant-in-Aid for Scientific Research from the Ministry of Education, Japan (No. 911503 and 01100).

REFERENCES

1. Terenin, A., and Roev, L., in "Proceedings of the Second International Congress on Catalysis, Paris," Vol. 2, p. 2183 (1961).
2. Kugler, E. L., Kokes, R. J., and Gryder, J. W., *J. Catal.* **36**, 142 (1975).
3. Arai, H., and Tominaga, H., *J. Catal.* **43**, 131 (1976).
4. Windhorst, K. A., and Lunsford, J. H., *J. Amer. Chem. Soc.* **97**, 1407 (1975).
5. Lunsford, J. H., *J. Chem. Phys.* **46**, 4347 (1967).
6. Lunsford, J. H., *J. Catal.* **14**, 379 (1969).
7. Niwa, M., Minami, T., and Murakami, Y., *Bull. Chem. Soc. Japan* **49**, 565 (1976).
8. Chao, C. C., and Lunsford, J. H., *J. Phys. Chem.* **76**, 1546 (1972); **78**, 1174 (1974).
9. Jermyn, J. W., Johnson, T. J., Vansant, E. F., and Lunsford, J. H., *J. Phys. Chem.* **77**, 2964 (1973).
10. Solymosi, F., and Kiss, J., *J. Catal.* **41**, 209 (1976).
11. Ogden, J. S., and Ricks, M. J., *J. Chem. Phys.* **53**, 896 (1970).
12. Kugler, E. L., Kadet, A. B., and Gryder, J. W., *J. Catal.* **41**, 72 (1976).
13. Lunsford, J. H., *J. Phys. Chem.* **72**, 2141 (1968).
14. Primet, M., Che, M., Naccache, C., Mathieu, M., and Imelik, B., *J. Chim. Phys. Physicochim. Biol.* **67**, 1629 (1970).
15. Kasai, P. H., and Bishop, R. J., Jr., *J. Amer. Chem. Soc.* **94**, 5560 (1972).
16. Kanzig, W., and Cohen, M. H., *Phys. Rev. Lett.* **3**, 509 (1959).
17. Shelef, M., and Otto, K., *J. Catal.* **10**, 408 (1968); **12**, 361 (1968).
18. Niiyama, H., Iida, H., and Echigoya, E., *Nippon Kagaku Kai-shi* **1975**, 1467.
19. Murakami, Y., Hayashi, K., Yasuda, K., Itoh, T., Minami, T., and Miyamoto, A., *Nippon Kagaku Kai-shi* **1977**, 173.
20. Fischer, L., *J. Mol. Spectrosc.* **40**, 414 (1971).